Pergamon

Int. J. Heat Mass Transfer. Vol. 38, No. 12, pp. 2259–2267, 1995

0017-9310/95 $9.50+0.00

0017-9310(94)00337-8

Evaporation of liquid droplets containing small solid particles

T. ELPERIN and B. KRASOVITOV

Pearlstone Center for Aeronautical Engineering Studies, Department of Mechanical Engineering, Ben-Gurion University of the Negev, P.O. Box 653, Beer-Sheva 84105, Israel

(*Received* 17 *February* 1994 *and in final form* 7 *October* 1994)

Abstract—Evaporation of a liquid droplet containing small solid particles (slurry droplets) is analyzed in a quasi-steady approximation. The developed model takes into account effects of compressibility and filtration of a gas–vapor mixture within the porous shell. It is shown that in the case of small temperature differences in the neighborhood of a slurry droplet at the second stage of drying (evaporation through a porous shell), the regime of slow evaporation and saturation (negligibly small drying rate) occurs. In the case of high temperature differences in the neighborhood of a slurry droplet at the second stage of drying, the pressure of the gas–vapor mixture within the porous shell significantly increases leading to the fragmentation of a porous shell. The comparison of the proposed model with the diffusion model, which neglects the Stefan's flux shows that the diffusion model incorrectly describes evaporation of a slurry droplet at the final stage of drying.

1. INTRODUCTION

Evaporation of droplets containing small solid particles (slurry droplets) is encountered in various engineering fields, e.g. pharmaceutical industry, bioengineering, food industry [1–3]. Coal–water slurries are used as a liquid fuel for boilers [4, 5]. Moreover aerosol generation of materials has seen many new developments in recent years. One of the new applications of this technology is spray pyrolysis. Spray pyrolysis is an aerosol process commonly used to form a wide variety of materials in powder form, including metals, metal oxides, nonoxide ceramics, superconducting materials, fullerenes, and nanophase materials [6]. In spite of the importance of slurry droplet evaporation for engineering applications there are few publications analyzing this problem. The purpose of this research is to develop a comprehensive model for slurry droplet evaporation and drying. In the literature the problem of evaporation of droplets containing small solid particles is treated with the aid of the two models:

(1) droplet with crust [7–10];
(2) droplet with bubble [11, 12].

Both models consider the evaporation and drying of slurry droplets to occur in two stages (see Fig. 1). During the first stage, immediately after the injection of a slurry droplet into the ambient hot air, the droplet is assumed to be composed mainly of liquid and its evaporation rate is assumed to be controlled by the gas phase resistance. During evaporation the amount of liquid mass, m_l, decreases while the solid mass remains constant and droplet diameter continuously shrinks. At some critical solid–liquid mass ratio (m_p/m_l), the discrete insoluble solid particles form an agglomerate (or cannot contract anymore), while the voids between particles are still filled with liquid. At this moment, which is assumed to occur at the prespecified critical solid–liquid mass ratio, the second stage of drying begins. In ref. [7] this critical mass ratio for coal–water and coal–lime slurry droplets was calculated to be 5.35. This value was obtained from a minimum void fraction attained in packing of spherical particles. Since the densities of solid particles and liquid may differ considerably, it is more convenient to employ the notion of the critical solid–liquid volume ratio $\delta = V_s/V_l$. The first stage of drying is assumed to occur when $\delta < \delta_c$ (where δ_c is value of critical solid–liquid volume ratio). When $\delta = \delta_c$ the second stage of drying begins.

During the second stage of drying the process is determined by the ambient conditions (ambient temperature, pressure etc.). If the ambient temperature is in the range 20–200°C, the drying rate is not large. In this case, evaporating liquid flows through the porous spherical shell between r_i and r_o, where r_i and r_o are inner and outer radii of the solid shell. Mass flux of the volatile species depends primarily on the permeability of the formed porous crust for the passage of vapor and heat and on the parameters of the ambient gas. In ref. [7] this flux was calculated from the following equation, which considers a Stefan-type diffusion:

$$\frac{dm_l}{dt}\frac{1}{4\pi\alpha^b}\left(\frac{1}{r_o}-\frac{1}{r_i}\right)=\frac{M_v D_v p_T}{R^* T_{ave}}\ln\frac{p_T-p_{vi}}{p_T-p_{vo}}. \quad (1)$$

In equation (1), α is the void fraction of the dry crust, and the exponent b is assumed to be equal to 1, T_{ave} is the average temperature defined as $T_{ave} = 0.5$

NOMENCLATURE

C_i	$= n_i/\Sigma_i n_i$ dimensionless concentration
D	diffusion coefficient
d	diameter
h	specific enthalpy
$\mathbf{j}_T$	density of heat flux
$\mathbf{j}_i$	density of mass flux of molecules of ith species
k	coefficient of thermal conductivity
K	permeability
L_v	latent heat of evaporation
m	mass
M	molecular mass
M_v	molar mass of the volatile species
n_i	concentration of ith species
p	pressure
Q_T	integral heat flux
Q_l	integral mass flux of vapor
r_i	inner radii of the solid shell in formula (1)
r_o	outer radii of the solid shell in formula (1)
r_g	radius of a gas bubble
R	radius of a droplet
R^*	universal gas constant
$R_{g,m}$	$= R^*/M$ gas constant of vapor–gas mixture
t	time
T	temperature
$\mathbf{u}$	superficial (Darcian) velocity
$\mathbf{v}$	velocity of the Stefan's flux
V	volume.

Greek symbols

α	void fraction in formula in equation (1)
δ	solid–liquid volume fraction
δ_i	initial volume fraction of solid particles
δ_c	critical value of solid–liquid volume fraction
ε	porosity
μ	viscosity
ρ	density
σ	coefficient of surface tension.

Subscripts

b	bubble
eff	effective value
i	ith species
l	liquid
m	mixture
p	particles
s	solid or value at the surface
1, 2	1st or 2nd species (1st species denotes a vapor)
∞	value at infinity.

Superscripts

(i)	value inside a porous shell
(e)	value outside a droplet or a porous shell.

$(T_o + T_i)$, p_{vl} and p_{vo} are the partial pressures of the vapor at the inner and outer surfaces of the dry spherical shell, respectively, p_{vi} is assumed to be saturation pressure of vapor at the wet core temperature, T_i, can be calculated from the energy equation, and p_T is the total pressure in the surrounding medium, M_v is a molar mass of the volatile species and D_v is a vapor–air diffusion coefficient.

In derivation of equation (1) it is assumed that, during the second stage (i.e. until porous solid core fragmentation), the value r_o is approximately equal to r_i. The mass flux through the porous core is determined by multiplying a mass flux through a single straight capillary channel by the void fraction of the dry crust. In this model it was assumed that the fragmentation occurs when the partial pressure of the water vapor at the wet interface equals the ambient atmospheric pressure. This limiting value is reached

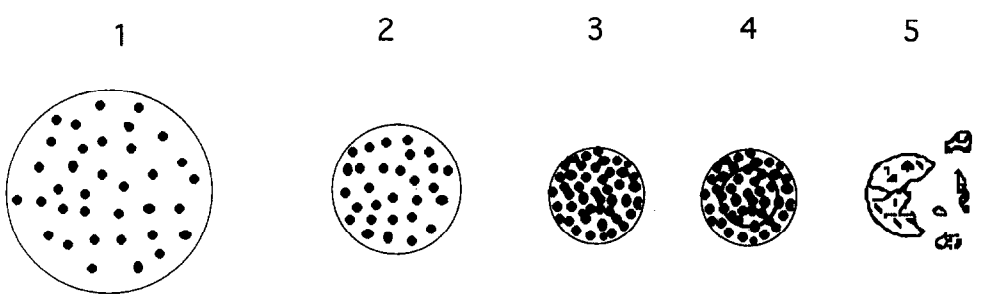

Fig. 1. Stages of drying of a slurry droplet. (1, 2) first stage of drying; (3, 4) second stage of drying; (5) stage of fragmentation.

within the slurry droplet since the crust temperature rises during the second stage of drying and the amount of evaporated water vapor cannot counterbalance the energy input [13–15].

The 'droplet with bubble' model was used in ref. [11] for the simulation of drying of a spherical droplet containing colloidal materials until a hollow sphere is formed. The model employs the Fickian transport equation for a hollow sphere. This equation was derived to describe the evaporation of moisture from a single, isolated spherical droplet containing colloidal particles. The obtained results are compared favorably with experimental data for the drying of single aqueous droplets containing skim milk.

The droplet with bubble model was applied in ref. [12] to assess the drying rate of a slurry droplet. It was suggested to replace the known relation for the evaporation rate of a pure liquid droplet by the following formulae:

$$\dot{m}_l = -\frac{\pi}{6}\rho_l \varepsilon_0 \frac{\mathrm{d}}{\mathrm{d}t}(d_i^3) \quad \text{(dry shell)}$$

$$\dot{m}_l = -\frac{\pi}{6}\rho_l \frac{\mathrm{d}}{\mathrm{d}t}[\varepsilon_c(d_{s,c}^3 - d_i^3) + \varepsilon_0 d_i^3] \quad \text{(wet shell)} \qquad (2)$$

where ε_0 and ε_c are initial volume fraction of liquid and critical volume fraction, respectively, and $d_{s,c}$ and d_i are outer and inner shell diameters, correspondingly.

In the case when drying occurs in a high temperature environment the first model ('droplet with crust') assumes that the temperature of the liquid within the core reaches the boiling point. A large amount of vapor is formed during this period and the internal pressure in a droplet increases. Depending on the permeability and mechanical properties of the formed crust, the droplet inflates, bursts or cracks. The latter model was used in ref. [8] for simulation of high temperature drying of droplet containing colloidal or dissolved nonvolatile substance.

In the 'droplet with bubble' model developed in refs. [11, 12] it is assumed that, since the liquid droplet is surrounded by a rigid shell during the second stage of drying, the continuous depletion of liquid due to gasification causes continuous expansion of a saturated vapor bubble inside the slurry core. Eventually the expanding gas bubble will rupture the porous crust. It is postulated that the slurry will continuously wet the inner surface of the shell, such that the vapor bubble is not in direct contact with the shell. Due to increasing pressure within the bubble, the pressure on the crust increases and the crust cracks.

Although both models (droplet with bubble and droplet with crust) attempt to explain the final stage of evaporation through porous shell (fragmentation) qualitatively, the nature of this phenomenon is not clear yet. To the best of our knowledge the model that allows correct description of the phenomena occurring during this stage has not been developed yet. Moreover, it can be seen from the above analysis that both available models have a rather limited range of applications.

In contrast to these models, the present model is based on exact conservation equations obtained by correct mean-value operation with effective heat and mass transfer coefficients. Furthermore the significant effects of compressibility and filtration of a gas–vapor mixture within the porous shell, disregarded in the previous models, are taken into account. It is shown that, when these effects are taken into account, the pressure inside a slurry droplet at the second stage of drying (evaporation through a porous shell) increases significantly. The latter phenomenon occurs during slurry droplet drying in a high temperature environment and may be a cause of a fragmentation of a porous shell. The developed approach also allows description of a wide variety of porous media forming a solid crust.

2. SLURRY DROPLET EVAPORATION

Consider a spherical droplet with radius R containing small solid particles and immersed into a stagnant binary gas mixture at a temperature T_∞, with concentration of volatile species $C_{1,\infty}(C_i = n_i/\sum_i n_i, n_i$ is the dimensionless concentration of the ith species, molecules of volatile species are denoted by index 1). Hereafter we assume the arbitrary temperature differences in the neighborhood of a slurry droplet.

The volume of a slurry droplet

$$V = V_l + V_s \qquad (3)$$

where V_s is the total volume of solid particles contained in the droplet and V_l is the volume of liquid. The total volume of solid particles

$$V_s = \delta_i V_0 \qquad (4)$$

where δ_i is the initial volume fraction of solid phase and V_0 is the initial volume of a slurry droplet. As was mentioned above, at the first stage of evaporation the solid porous crust is formed when the solid–liquid volume ratio V_s/V_l is equal to critical value δ_c. The value of the critical parameter δ_c can be obtained from a minimum void fraction attained in packing of spherical particles. The porosity of spherical particles packing is determined as follows:

$$\varepsilon = \frac{V_l}{V_l + V_s}. \qquad (5)$$

Thus using equation (5) we can obtain the critical solid–liquid volume ratio:

$$\delta_c = \frac{V_s}{V_l} = \frac{1-\varepsilon}{\varepsilon}. \qquad (6)$$

In the case of packing of spherical particles, the value of porosity is known to vary in the range 0.36–0.44. It has been established that porosity is equal to 0.36 for a well shaken granular medium (see pp. 19–20 in ref. [16] for an example). Therefore in the case

of a slurry droplet evaporation, the porosity of a porous shell can vary in the range 0.39–0.44.

Thus the initial solid–liquid volume ratio in the slurry droplet is assumed to be $V_s/V_l < \delta_c$. The process of evaporation of slurry droplets is modeled in two stages. Consider the first stage of drying when $V_s/V_l < \delta_c$.

As discussed above, during this stage the droplet is assumed to be composed mainly of water and the evaporation rate is controlled by the gas phase resistance. This stage of drying can be described by the system of mass and energy conservation equations:

$$\operatorname{div} \mathbf{j}_i^{(e)} = 0 \quad \operatorname{div} \mathbf{j}_T^{(e)} = 0 \tag{7}$$

where

$$\mathbf{j}_i^{(e)} = \rho_i^{(e)} \mathbf{v}^{(e)} - \frac{n^2 m_i m_j}{\rho} D^{(e)} \nabla C_i^{(e)}$$

$$\mathbf{j}_T^{(e)} = \sum_i h_i \mathbf{j}_i^{(e)} - k^{(e)} \nabla T^{(e)}$$

$$i, j = 1, 2; i \neq j$$

with the boundary conditions

$$T^{(e)}|_{r=R} = T_s \tag{8}$$

$$C_1^{(e)}|_{r=R} = C_{1,s}^{(e)}(T_s) \tag{9}$$

$$((L_v - h_1)\mathbf{j}_1^{(e)} + \mathbf{j}_T^{(e)})|_{r=R} = 0 \tag{10}$$

where $C_i^{(e)} = n_i / \sum_i n_i$ is a dimensionless concentration of the ith species in the neighborhood of a droplet (i, $j = 1, 2$; $i \neq j$ and indexes 1 and 2 denote volatile and external gas species, correspondingly), $T^{(e)}$ is temperature outside the droplet, $k^{(e)}$ is heat conductivity of the ambient medium, D is diffusion coefficient, L_v is latent heat of evaporation, R is the radius of a droplet. Subscript s denotes the value at the surface, and superscript (e) denotes value outside the droplet. The radiation heat flux in the boundary condition (10) is not taken into account. As it was shown in ref. [19], the effect of radiation heat transfer is significant for liquid droplets with the radii 0.5 mm and larger and high ambient temperature.

Conditions at infinity are

$$T^{(e)}|_{r\to\infty} \to T_\infty, \quad C_1^{(e)}|_{r\to\infty} \to C_{1,\infty}. \tag{11}$$

In the case of arbitrary temperature differences in the neighborhood of a slurry droplet, the system of equations (7) with the boundary conditions (8)–(10) and conditions at infinity (11) yields the following expressions for temperature and dimensionless concentration of volatile species distributions [19]:

$$\int_{T_\infty}^{T^{(e)}} k^{(e)} \, dT^{(e)} = \frac{R}{r} \int_{T_\infty}^{T_s} k^{(e)} \, dT^{(e)} \tag{12}$$

$$C_1 = C_{1,\infty} + (C_{1,s} - C_{1,\infty}) \frac{\int_{T_\infty}^{T^{(e)}} \frac{k^{(e)}}{nD} dT^{(e)}}{\int_{T_\infty}^{T_s} \frac{k^{(e)}}{nD} dT^{(e)}}. \tag{13}$$

The unknown temperature at the droplet's surface T_s in formulas (12)–(13) can be found from the following transcendental equation which is obtained by substitution of solutions (13) into the boundary condition (10):

$$\int_{T_\infty}^{T_s} \frac{k^{(e)}}{nD} dT^{(e)} + L_v m_1 (C_{1,s} - C_{1,\infty}) = 0 \tag{14}$$

where $C_{1,s}(T_s)$ is determined by the Clapeyron–Clausius equation:

$$C_{1,s}(T_s) = C_1(T_0) \exp\left(\frac{L_v M_v}{R^*}\left(\frac{1}{T_0} - \frac{1}{T_s}\right)\right).$$

In the last expressions M_v is molecular mass of volatile species, $C_1(T_0)$ is density of saturated vapor at temperature T_0, and R^* is the universal gas constant.

The integral heat and mass fluxes can be found as follows:

$$Q_1 = \oint_S m_1 D^{(e)} n \nabla C_1^{(e)} \, dS \quad Q_T = \oint_S k^{(e)} \nabla T^{(e)} \, dS. \tag{15}$$

Then using solutions (12)–(13), the following expressions for heat and mass fluxes are obtained:

$$Q_T = 4\pi R \int_{T_\infty}^{T_s} k^{(e)} \, dT^{(e)}$$

$$Q_1 = 4\pi R m_1 (C_{1,s}(T_s) - C_{1,\infty}) \frac{\int_{T_\infty}^{T_s} k^{(e)} \, dT^{(e)}}{\int_{T_\infty}^{T_s} \frac{k^{(e)}}{nD^{(e)}} dT^{(e)}}. \tag{16}$$

Finally the radius of an evaporating droplet can be found from the following differential equation:

$$\frac{dm_l^*}{dt} = -Q_1 \tag{17}$$

where m_l^* is the mass of liquid and t is the time.

Once the solid–liquid mass ratio in the slurry droplet reaches the critical value, the second stage of drying begins. As is seen from Fig. 2, during this stage the droplet can be viewed as composed of two regions: (a) central spherical wet porous kernel, and (b) dry porous shell surrounding this kernel. Thus the boundary value problem must be formulated in three domains: wet porous kernel, porous shell and ambient vapor–gas mixture.

Assume that the wet kernel is fully saturated with liquid and saturation is equal to zero within the porous shell. Since the effective coefficient of heat conductivity within the wet kernel is much greater than

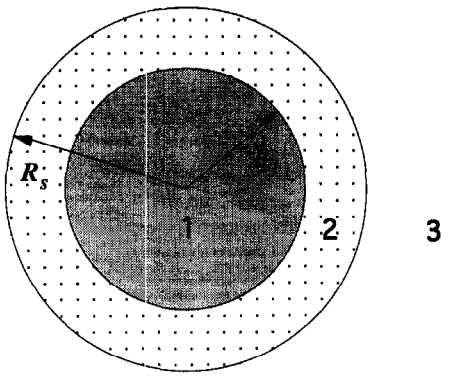

Fig. 2. Model of evaporating of a slurry droplet. (1) Wet kernel; (2) porous shell; (3) ambient gas–vapor mixture.

the coefficient of heat conductivity within the porous shell, we can assume that the temperature at the liquid interface is equal to the temperature within the liquid kernel. Thus under the above assumptions the system of mass and energy conservation equations inside and outside the porous crust reads:

$$\operatorname{div}(\rho^{(i)}\mathbf{v}^{(i)}) = 0 \tag{18}$$

$$\operatorname{div}\mathbf{j}_i^{(i)} = 0 \tag{19}$$

$$\operatorname{div}\mathbf{j}_T^{(i)} = 0 \tag{20}$$

$$\varepsilon\mathbf{v}^{(i)} = -\frac{K}{\mu}\nabla p^{(i)} \tag{21}$$

$$\operatorname{div}(\rho^{(e)}\mathbf{v}^{(e)}) = 0 \tag{22}$$

$$\operatorname{div}\mathbf{j}_i^{(e)} = 0 \tag{23}$$

$$\operatorname{div}\mathbf{j}_T^{(e)} = 0 \tag{24}$$

where

$$\mathbf{j}_i^{(i)} = \rho_i^{(i)}\mathbf{v}^{(i)}\varepsilon - D_{\text{eff}}^{(i)}\frac{(n_i^{(i)}+n_j^{(i)})^2 m_i m_j}{\rho^{(i)}}\nabla C_i^{(i)} \tag{25}$$

$$\mathbf{j}_T^{(i)} = \sum_i h_i\mathbf{j}_i^{(i)} - k_{\text{eff}}^{(i)}\nabla T^{(i)} \tag{26}$$

$$\mathbf{j}_i^{(e)} = \rho_i^{(e)}\mathbf{v}^{(e)} - D^{(e)}\frac{(n_i^{(e)}+n_j^{(e)})^2 m_i m_j}{\rho^{(e)}}\nabla C_i^{(e)} \tag{27}$$

$$\mathbf{j}_T^{(e)} = \sum_i h_i\mathbf{j}_i^{(e)} - k^{(e)}\nabla T^{(e)} \tag{28}$$

where

$$\varepsilon\mathbf{v}^{(i)} = \mathbf{u} = \frac{\rho_1^{(i)}u_1 + \rho_2^{(i)}u_2}{\rho}$$

is a superficial (Darcian) velocity (averaged over entire pore volume), ρ_i is the density of ith species ($i, j = 1, 2$; $i \neq j$ and indexes 1 and 2 denote volatile and external gas species, correspondingly), h_i is the enthalpy of ith species, superscripts (e) and (i) denote the value within and outside the porous shell, μ is viscosity coefficient, and K is a permeability coefficient. The permeability of a porous shell can be found from the Carman–Kozeni equation which is proved to be accurate for randomly packed spherical particles [16] and is reasonably accurate for various types of porous media:

$$K = \frac{d^2\varepsilon^3}{180(1-\varepsilon)^2}$$

where d is an average hydraulic diameter of particles.

The boundary conditions for the system of equations (18)–(28) are

$$T^{(e)}|_{r=R_s} = T^{(i)}|_{r=R_s} = T_s \tag{29}$$

$$C_1^{(e)}|_{r=R_s} = C_1^{(i)}|_{r=R_s} = C_{1,s} \tag{30}$$

$$p^{(e)}|_{r=R_s} = p^{(i)}|_{r=R_s} = p_\infty \tag{31}$$

$$\left(\rho_1^{(i)}v_r^{(i)} - \frac{D_{\text{eff}}^{(i)}}{\varepsilon}\frac{\partial C_1^{(i)}}{\partial r}\right)\Bigg|_{r=R_s} = \left(\rho_1^{(e)}v_r^{(e)} - D^{(e)}\frac{\partial C_1^{(e)}}{\partial r}\right)\Bigg|_{r=R_s} \tag{32}$$

$$\left(h_1 j_{r,1}^{(i)} - k_{\text{eff}}^{(i)}\frac{\partial T^{(i)}}{\partial r}\right)\Bigg|_{r=R_s} = \left(\varepsilon h_1 j_{r,1}^{(e)} - \varepsilon k^{(e)}\frac{\partial T^{(e)}}{\partial r}\right)\Bigg|_{r=R_s} \tag{33}$$

$$\mathbf{j}_T^{(i)}|_{r=R_l} + (L_v - h_1)\mathbf{j}_1^{(i)}|_{r=R_l} = 0 \tag{34}$$

$$T^{(i)}|_{r=R_l} = T_l \tag{35}$$

$$C_1^{(i)}|_{r=R_l} = C_{1,l}^{(i)}(T_l) \tag{36}$$

$$p^{(i)}|_{r=R_l} = p_l. \tag{37}$$

In the boundary conditions (29)–(37) R_s is the radius of the porous shell, R_l is the radius of the boundary of liquid interface and T_l is the temperature at the boundary of liquid interface and $C_{1,l}^{(i)}(T_l)$ can be found from Kelvin's equation:

$$C_{1,l}^{(i)}(T) = C_1^{(0)}(T)\exp\left\{-\frac{2\sigma_{l,g}\cos\vartheta V_l}{R^*\rho_k T}\right\}$$

where $C_{1,l}^{(i)}(T)$, $C_1^{(0)}(T)$ are concentrations under distorted and flat surfaces, respectively, $\sigma_{l,g}$ is surface tension at the liquid–gas boundary, ρ_k is radius of a capillary pore and ϑ is the contact angle. The radius of capillary pore in the case of a random packing of monosized spheres is determined as the value of the order of the sphere's radius. The contact angle in Kelvin's equation can be obtained from Young's equation:

$$\cos\vartheta = (\sigma_{s,g} - \sigma_{s,l})/\sigma_{l,g}$$

where $\sigma_{s,g}$, $\sigma_{s,l}$ and $\sigma_{l,g}$ are coefficients of surface tension at the solid–gas, solid–liquid and liquid–gas interfaces, correspondingly.

In expressions (25), (26), (32), (33) the coefficients $D_{\text{eff}}^{(i)}$, $k_{\text{eff}}^{(i)}$ are effective diffusion coefficient and effective thermal conductivity, respectively.

Conditions at infinity are given by expression (11).

As can be seen from equations (19) these equations can be easily integrated to yield:

$$j_i^{(i)} = \frac{A_i}{r^2} \tag{38}$$

where $A_i = (Q_i^{(i)}/4\pi)$ and $Q_i^{(i)}$ is a constant integral mass flux of the ith species. Since the flux of gas species through liquid interface is equal to zero (i.e. $j_2^{(i)} = Q_i^{(i)}/4\pi r^2 = 0$) and the total dimensionless concentration of binary mixture is equal to 1 (i.e. $C_1^{(i)} = 1 - C_2^{(i)}$), then from equations (18)–(20), taking into account spherical symmetry of the problem, we obtain:

$$v_r^{(i)}(1-C_1^{(i)}) + D_{eff}^{(i)} \frac{n^{(i)} m_1}{\rho^{(i)}} \frac{dC_1^{(i)}}{dr} = 0 \tag{39}$$

$$\rho^{(i)} v_r^{(i)} = \frac{Q_c^{(i)}}{4\pi r^2}. \tag{40}$$

Substituting equation (38) into equation (26) and integrating yields:

$$k_{eff}^{(i)} \frac{dT^{(i)}}{dr} = \frac{Q_1^{(i)} h_1 - Q_T^{(i)}}{4\pi r^2}. \tag{41}$$

Since temperature $T^{(i)}$ depends on coordinate r only, we can choose $T^{(i)}$ as an independent variable and then, using equations (41) and (40), equation (39) becomes:

$$\frac{\rho^{(i)}}{m_1} \frac{Q_1^{(i)}}{(Q_1^{(i)} h_1 - Q_T^{(i)})}(1-C_1^{(i)}) + \frac{n^{(i)} D_{eff}^{(i)}}{k_{eff}^{(i)}} \frac{dC_1^{(i)}}{dT^{(i)}} = 0. \tag{42}$$

During the first stage of a slurry droplet evaporation the vapor leaves the surface of a slurry droplet by diffusion and convection. In contrast to the first stage of drying, during the second stage filtration is a dominating mechanism of mass transfer. In this case the concentration of volatile (vapor) species within the porous shell can be significant. Therefore the coefficients of heat and mass transfer depend on temperature and concentration of gas species. Then equation (42) must be integrated, taking into account the following dependence of the heat and mass transfer coefficients:

$$D_{eff}^{(i)} = D_T^{(i)}(T^{(i)}) D_c^{(i)}(C_1), \quad k_{eff}^{(i)} = k_T^{(i)}(T^{(i)}) k_c^{(i)}(C_1) \tag{43}$$

where $D_T^{(i)}(T^{(i)})$ and $k_T^{(i)}(T^{(i)})$ are functions depending on temperature only and $D_c^{(i)}(C_1)$ and $k_c^{(i)}(C_1)$ are functions depending on concentration only. Then using equation (43) and boundary conditions (29), (30) and (35), (36) after integrating (42) we obtain:

$$\frac{Q_1^{(i)}}{Q_1^{(i)} h_1 - Q_T^{(i)}} \int_{T_1}^{T_s} \frac{k_T^{(i)}}{n^{(i)} D_T^{(i)}} dT^{(i)} = m_1 \int_{C_{1,1}}^{C_{1,s}} \frac{\lambda_c}{C_1 - 1} dC_1 \tag{44}$$

where $\lambda_c = D_c^{(i)}(C_1)/k_c^{(i)}(C_1)$ and functions $D_c^{(i)}(C_1)$ and $k_c^{(i)}(C_1)$ can be calculated as functions of $T^{(i)}$ which depends on C_1. In the case of gas mixtures with approximately equal molecular weights the ratio $\lambda_c = D_c^{(i)}(C_1)/k_c^{(i)}(C_1) \approx 1$. Thus the right hand side of equation (44) can be integrated and yields:

$$\frac{Q_1^{(i)}}{Q_1^{(i)} h_1 - Q_T^{(i)}} \int_{T_1}^{T_s} \frac{k_T^{(i)}}{n^{(i)} D_T^{(i)}} dT^{(i)} = m_1 \ln \left| \frac{C_{1,s} - 1}{C_{1,1} - 1} \right|. \tag{45}$$

Using the linear relation with saturation we can define the effective diffusion coefficient $D_T^{(i)}$ as follows [16]:

$$D_T^{(i)} = D(T^{(i)}) \frac{2\varepsilon}{3-\varepsilon}(1-s).$$

As was noted above, the wet kernel is saturated fully with the liquid (i.e. $s = 1$) and saturation is equal to zero (i.e. $s = 0$) within the porous shell. In this case a convenient and relatively accurate correlation for effective thermal conductivity was suggested by Krupitczka [17]:

$$k_T^{(i)} = k_f \left(\frac{k_s}{k_f} \right)^{0.280 - 0.757 \log \varepsilon - 0.057 \log (k_s/k_f)}$$

or Batchelor and O'Brien's [18] correlation for the special case of point contact and high k_s/k_f:

$$k_T^{(i)} = k_f \left(4 \ln \frac{k_s}{k_f} - 11 \right)$$

where $k_f = k_f(T^{(i)})$ is thermal conductivity of fluid and k_s is thermal conductivity of the solid phase.

As can be seen from Fig. 3, in the case when porosity $\varepsilon = 0.4$, Krupiczka's and Batchelor and O'Brien's correlations for a shell composed of coal particles in an air matrix approximately coincide.

From equation (41), using boundary condition (29), we obtain:

$$\int_{T_1}^{T_s} k_T^{(i)} dT^{(i)} = \frac{(R_s - R_1)}{R_1 R_s}(h_1 Q_1^{(i)} - Q_T^{(i)}). \tag{46}$$

Substituting equation (40) into equation (21) and choosing $T^{(i)}$ as an independent variable after inte-

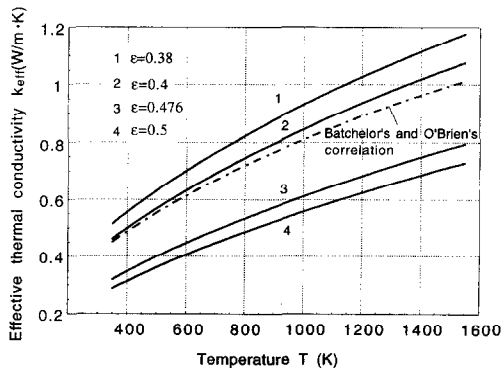

Fig. 3. Comparison of the dependence effective thermal conductivity vs ambient temperature between Krupiczka's and Batchelor–O'Brien's correlations.

grating equation (21) with the boundary conditions (29), (31), (35) and (37), we find that

$$p_l^2 = p_\infty^2 + 2\frac{Q_l^{(i)}}{h_l Q_l^{(i)} - Q_T^{(i)}} \frac{R_{g,m}}{K} \int_{T_l^{(i)}}^{T_s} k_T^{(i)} T^{(i)} \mu(T^{(i)})\, dT^{(i)} \tag{47}$$

where $R_{g,m} = R^*/M$ is a gas constant of a vapor–gas mixture and M is a molar mass of the mixture which is defined as follows: $M = M_1 M_2/((M_2 - M_1)\bar{C}_1 + M_1)$, $\bar{C}_1$ is an average concentration of the first species within the porous shell. In the following we assume the power dependence of function $\mu(T^{(i)})$ in expression (47) (i.e. $\mu(T) = \mu_\infty(T/T_\infty)^\omega$). Integrating (20) with the boundary condition (34) yields:

$$Q_T^{(i)} + (L_v - h_l)Q_l^{(i)} = 0. \tag{48}$$

The solution of equations (22)–(24) with boundary conditions (29), (30), (32), (33) and conditions at infinity (11) can be found similar to the previous solution for a wet kernel and reads:

$$R_s \int_{T_s}^{T_\infty} k^{(e)}\, dT^{(e)} = h_l Q_l^{(e)} - Q_T^{(e)} \tag{49}$$

$$C_{1,s} = C_{1,\infty} + \frac{Q_l^{(e)} C_{2,\infty}}{Q_l^{(e)} h_l - Q_T^{(e)}} \int_{T_\infty}^{T_s} \frac{k^{(e)}}{n^{(e)} D^{(e)}}\, dT^{(e)} \tag{50}$$

$$Q_l^{(e)} = \varepsilon Q_l^{(i)} \tag{51}$$

$$Q_T^{(e)} = \varepsilon Q_T^{(i)}. \tag{52}$$

In equation (50) was took into account that, at the outside of a porous shell, the concentration differences in the neighborhood are small. Thus the system of equations (45)–(52) is a closed system of algebraic equations for determination of unknown constants $T_l, T_s, C_{1,s}, p_l, Q_l^{(i)}, Q_T^{(i)}, Q_l^{(e)}, Q_T^{(e)}$.

Finally, the radius of evaporating internal liquid kernel can be found from the following differential equation:

$$\frac{4}{3}\pi\rho_l \varepsilon \frac{dR_l^3}{dt} = -Q_l^{(i)} \tag{53}$$

where ρ_l is the density of liquid and t is the time.

3. RESULTS AND DISCUSSION

The developed mathematical model of vaporization of slurry droplets in the case of arbitrary temperature differences in the neighborhood of a slurry droplet was applied to study a process of evaporation of a coal–water slurry droplet in a binary gas mixture. The results are presented for small ($T_\infty = 293$ K) and large ($T_\infty = 450$ K) temperature differences in the neighborhood of the slurry droplet and various values of initial volume fraction of solid phase, permeability and concentration of a volatile species in an ambient gas. In contrast to the previous models, the present model allows description of the increase of pressure within the porous shell, which is the cause of its fragmentation at the second stage of drying.

As mentioned above, the first stage of drying occurs when the value of solid–liquid volume ratio δ is less than critical parameter δ_c. When δ is equal to δ_c the porous shell with radius of R_s is formed and the second stage of drying begins. Using equations (4)–(6) the radius R_s of the porous shell can be determined as follows:

$$R_s = R_0^3 \cdot \sqrt{\frac{\delta_i}{1-\varepsilon}}$$

where R_0 is the initial radius of slurry droplet.

The results of numerical calculations of the dependence of liquid interface radius vs time of evaporation, t, for slurry droplets with initial radii 200 μm and various values of initial volume fraction of the particles are shown in Fig. 4. The results were obtained for ambient temperature, $T_\infty = 293$ K, concentration of volatile species, $C_{1,\infty} = 0.015$, porosity, $\varepsilon = 0.4$, and permeability, $K = 3.6 \times 10^{-14}$ m^2. The curves are plotted for initial solid fraction, $\delta = 0.4$, 0.2 and 0.1 and for a pure liquid droplet. The calculations show that the increase of pressure in this case does not exceed 0.01%. Thus in a case of small temperature differences in the neighborhood of a slurry droplet the fragmentation of a porous shell does not occur.

It is well known that the diffusion regime of evaporation occurs in the case when relative differences of concentration of volatile species in the neighborhood of a gas–vapor interface are small. In the case of evaporation of a pure liquid droplet immersed into an ambient gas this regime occurs for a wide range of ambient temperatures, and distribution of concentration in the neighborhood of the gas–liquid interface can be calculated using diffusion approximation (13). Thus at the first stage of drying when a slurry droplet is composed mainly of water, the diffusion approximation is valid. At the second stage when the vapor flows into the ambient gas through the porous shell in the external domain, the diffusion approximation for the concentration distribution (50) is valid

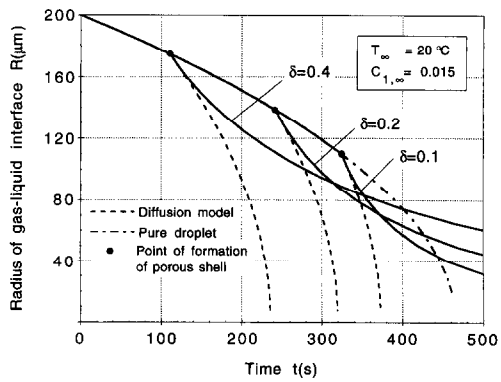

Fig. 4. Radius of gas–liquid interface vs time (solid lines—present model, dashed lines—diffusion model and pure liquid droplet).

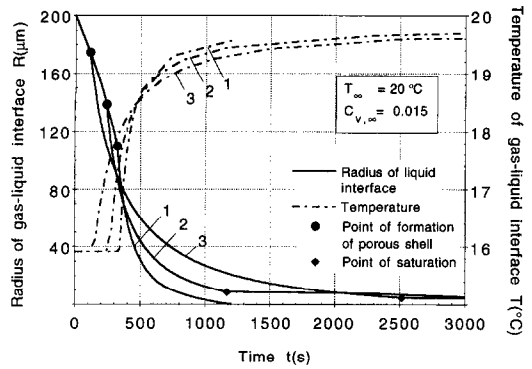

Fig. 5. Radius of gas–liquid interface and temperature at the gas–liquid interface vs time (small temperature differences in the neighborhood of a slurry droplet). (1) $\delta = 0.4$; (2) $\delta = 0.2$; (3) $\delta = 0.1$.

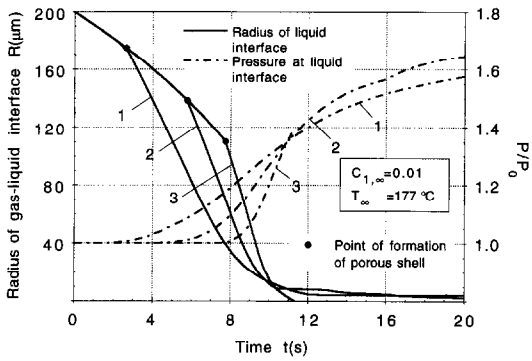

Fig. 6. Radius of gas–liquid interface and ratio p_l/p_0 vs time (high temperature differences in the neighborhood of a slurry droplet). (1) $\delta = 0.4$; (2) $\delta = 0.2$; (3) $\delta = 0.1$.

too, but inside the porous shell this approximation can be used only in some limited cases. The comparison of obtained results with the diffusion approximation (dashed lines in Fig. 4) shows that the diffusion regime occurs in the case of very small values of solid fraction.

The results of numerical calculations on the dependence of liquid interface radius and dependence of temperature vs time of evaporation, t, for slurry droplets with initial radii 200 μm and various values of initial volume fraction of the particles are shown in Fig. 5. The results were obtained for ambient temperature, $T_\infty = 293$ K, concentration of volatile species, $C_{1,\infty} = 0.015$, porosity, $\varepsilon = 0.4$, and permeability, $K = 3.6 \times 10^{-14}$ m^2. The curves 1–3 are plotted for the solid fraction $\delta = 0.1, 0.2$ and 0.4 correspondingly. As can be seen from these plots, in the case of evaporation of a slurry droplet with a large value of solid fraction at the final stage of drying, the porous shell is saturated with vapor. As a result of this effect the rate of evaporation of a slurry droplet with large solid fraction significantly decreases at the final stage of evaporation.

The results of calculation of the dependence of the radius of a gas–liquid interface and p_l/p_0 (where p_0 is normal atmospheric pressure $p_0 = 101\,325$ Pa) on time are shown in Fig. 6. As is seen from these plots,

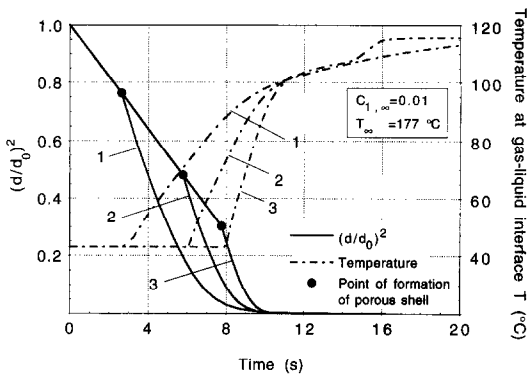

Fig. 7. Radius of a gas–liquid interface and temperature at the gas–liquid interface vs time (high temperature differences in the neighborhood of a slurry droplet). (1) $\delta = 0.4$; (2) $\delta = 0.2$; (3) $\delta = 0.1$.

during the second stage of drying the pressure at the gas–liquid interface increases significantly and it is more than likely that this is a cause of the fragmentation of a porous shell.

The boiling inside a wet kernel is supposed by some authors (see ref. [8] for example) to cause fragmentation of a porous shell. As can be seen from Fig. 7, the temperature at the gas–liquid interface is indeed above boiling point. However, simultaneously with the increase of temperature, the pressure within the porous shell also increases. As can be seen from Figs. 6 and 7, the temperature at the gas–liquid interface $T_l = 110$°C corresponds to pressure 154 014 Pa. It is well known that boiling occurs when a radius of a bubble within the liquid is greater then a critical radius. The growth of a vapor bubble in a liquid is controlled by three factors: the differences between liquid temperature and temperature at the bubble's surface ($T_l > T_{b,s}$), the surface tension, and the vapor pressure. The bubble surface temperature T_s can be found from Clapeyron–Clausius equation:

$$p(T_{b,s}) = p_0 \exp\left(\frac{L_v M_v}{R^*}\left(\frac{1}{T_0} - \frac{1}{T_{b,s}}\right)\right)$$

where $p(T_{b,s}) = p_b$ (p_b is the pressure within the bubble) can be determined as follows

$$p(T_{b,s}) = p_b = p_l + \frac{2\sigma}{r_g}.$$

In the last expression p_l is the pressure of liquid and σ is the surface tension. If we assume that the radius of a bubble is equal to an average radius of a pore ($\propto 1$ μm) and it is immersed into a domain saturated only by liquid (liquid kernel) with surface tension coefficient $\sigma = 0.58$ N m^{-1}, then p_b is equal to 269 524.5 Pa. Thus, using the Clapeyron–Clausius equation we obtain the condition of bubble growth as $T_{b,s} > 128.8$°C. The above calculations show that the temperature at the gas–liquid interface is less then the boiling temperature at a given pressure ($T_l < T_s$) and boiling inside a wet kernel does not occur.

Notably large temperature gradients inside a slurry droplet ($\nabla T \propto 3.5 \times 10^5$ K/m) result in a large thermal stress inside the porous shell. The fragmentation of the porous shell is caused most likely by the combined effects of these high thermal stresses and high internal pressure.

Variation of $(d/d_0)^2$ vs time of evaporation, t, for slurry droplets with initial diameter 400 μm and various values of initial volume fraction of the particles is shown in Fig. 7. The results were obtained for ambient temperature, $T_\infty = 450$ K, concentration of volatile species, $C_{1,\infty} = 0.01$, porosity, $\varepsilon = 0.4$, and permeability, $K = 3.6 \times 10^{-14}$ m^2. The curves 1–3 are plotted for the solid fraction $\delta = 0.1$, 0.2 and 0.4, correspondingly. As is seen from these plots, at the second stage of drying the d^2-law, which is perfectly true for evaporation of pure liquid droplets, is not valid anymore.

4. CONCLUSIONS

The 'wet kernel' model for slurry droplet drying is suggested. Evaporation of a liquid–solid slurry droplet in the case of arbitrary temperature differences in the neighborhood of the droplet is analyzed in a quasi-steady approximation. Notably compressibility and filtration of a gas–vapor mixture within the porous shell have significant effects upon the slurry droplet evaporation. In contrast to the existing models (droplet with crust and droplet with bubble), it is shown that, in the case of large temperature differences during the second stage of drying (evaporation through a porous shell), the pressure of gas–vapor mixture within a porous shell increases significantly and depends on the ambient temperature, initial solid fraction, porosity and permeability. It is suggested that increase of pressure gradient during the second stage of drying is the cause of fragmentation of a porous shell. It is shown that, in the case of considered temperature differences in the neighborhood of a slurry droplet, boiling inside the porous shell does not occur. The process of boiling inside the porous shell at the second stage of drying is a considerably more complicated phenomenon and is the subject of an ongoing investigation.

Acknowledgements—The work was supported in part by Israel Ministry of Science and Arts.

REFERENCES

1. K. Masters, Spray drying, *Adv. Drying* **1**, 269–298 (1980).
2. C. J. King, T. G. Kieckbush, C. G. Greenwald, Food-quality factors in spray drying, *Adv. Drying* **3**, 71–120 (1984).
3. M. Rosenberg, I. J. Kopelman and Y. Talmon, Factors affecting retention in spray-drying microencapsulation volatile materials, *J. Agric. Fd Chem.* **38**, 1288–1294 (1990).
4. C. B. Henderson, R. S. Scheffe, E. T. McHalle, Coal-water slurries—a low-cost liquid fuel for boilers, *Energy Prog.* **3**(2), 69–75 (1983).
5. B. G. Miller Coal-water slurry fuel utilization in utility and industrial boilers, *Chem. Engng Prog.* **85**(3), 29–38 (1989).
6. A. Gurav, T. Codas, T. Pluym and Y. Xiong, Aerosol processing of materials, *Aerosol Sci. Technol* **19**(4), 407–452 (1993).
7. N. Abuaf and F. W. Staub, Drying of liquid-solid slurry droplets, *Drying '86, Proc. Fifth Int. Symp. on Drying*, Vol. 1, pp. 277–284, Massachusetts Institute of Technology (1986).
8. Srdjan Nešič, The evaporation of single droplets—experiments and modeling. In *Drying '89* (Edited by A. S. Mujumdar and M. Roques), pp. 386–393 Hemisphere, NY (1989).
9. T. O. K. Audu and J. V. Jeffreys, The drying of drops of particulate slurries, *Trans. INSTN Chem. Engrs* **53**, 165–172 (1975).
10. H. W. Cheong, G. V. Jeffreys and C. J. Mumford, A receding interface model for the drying of slurry droplets, *A.I.Ch.E. J.* **32**(8), 1334–1346 (1986).
11. Y. Sano and K. B. Keey, The drying of a spherical particle containing colloidal material into a hollow sphere, *Chem. Engng Sci.* **37**(6), 881–889 (1982).
12. A. Lee and C. K. Law, Gasification and shell characteristics in slurry droplet burning, *Combust. Flame* **85**, 77–93 (1991).
13. F. Takahashi, I. J. Heilweil and F. L. Dryer, Disruptive burning mechanism of free slurry droplets, *Combust. Sci. Technol.* **65**, 161–165 (1989).
14. D. J. Maloney and J. F. Spann, Evaporation, agglomeration and explosive boiling characteristics of Coal-Water fuels under intense heating conditions, *22nd Symp. (Int.) Combustion*, The Combustion Institute, pp. 1999–2008 (1988).
15. R. W. Lyszkowski and Y. T. Chao, Comparison of Stefan model with two-phase model of coal drying, *Int. J. Heat Mass Transfer* **27**(8), 1157–1169 (1984).
16. M. Kaviany, *Principles of Heat Transfer in Porous Media*. Springer, New York (1991).
17. R. Krupitczka, Analysis of thermal conductivity in granular materials, *Int. Chem. Engng* **7**, 122–144 (1967).
18. G. K. Batchelor and R. W. O'Brien, Thermal or electrical conduction through a granular material, *Proc. R. Soc. Lond. A* **355**, 313–333 (1977).
19. T. Elperin and B. Krasovitov, Radiation, thermal diffusion and kinetic effects in evaporation and combustion of large size and moderate size fuel droplets, *Int. J. Heat Mass Transfer* **38**(3), 409–418 (1995).